ELSEVIER

Journal of Power Sources 92 (2001) 108–119

JOURNAL OF POWER SOURCES

www.elsevier.com/locate/jpowsour

Development of 1 kW h class lithium ion battery for power storage

Masatoshi Majima[a,*], Satoshi Ujiie[b], Eriko Yagasaki[b], Shinji Inazawa[a], Kenji Miyazaki[a]

[a]*Osaka R&D Laboratory, Sumitomo Electric Industries Ltd., 1-1-3 Shimaya, Konohana-ku, Osaka 554-0024, Japan*
[b]*Technical Research Center, The Kansai Electric Power Company Inc., 3-11-20 Nakoji, Amagasaki, Hyogo 661-0974, Japan*

Received 30 September 1999; received in revised form 20 April 2000; accepted 24 May 2000

Abstract

With the aim of developing 1 kW h class lithium ion batteries with long life and high efficiencies, we trial manufactured batteries that were fabricated using $LiCoO_2$ and natural graphite as cathode and anode materials, respectively, with 1 M $LiPF_6$ diluted by EC/DEC as an electrolyte. Fundamental studies necessary for the development of a large-scale battery consisting of laminated large electrodes were conducted, examining various factors. These factors were selected from the observations of batteries dismantled after the battery life reached an end point. The construction of the batteries was based on the results of fundamental research done to elucidate the problems encountered in the present study. We achieved 543 cycles with high efficiencies with the fourth battery. It is noteworthy that technical factors such as homogeneous impregnation of the electrolyte into the electrode laminates and maintenance of uniform conditions of laminates by the control of expansion and contraction accompanied with charge and discharge, respectively, were very important for the long life of large-scale lithium ion batteries. © 2001 Elsevier Science B.V. All rights reserved.

Keywords: Lithium ion battery; $LiCoO_2$; Electric power storage; Natural graphite

1. Introduction

The electricity consumption has been increasing steadily in Japan [1]. In consuming electricity, daily and seasonal differences of the consumption have been increased, and the mean annual percent load has decreased year by year to <60% [2].

Electricity, however, is difficult to be stored. Since electric power generating facilities, sufficient to supply the peak demand are needed, the net working rate of the facilities is reduced. If surplus electricity during the nighttime can be stored and released during the daytime, i.e. load-leveling, the average utilization of electric power generating facilities can be improved. Storage of electricity by secondary batteries is one of the most promising way of the load leveling.

The size of batteries for the load leveling is much different and is dependent on their usage [3]. The batteries used on the supplier are of a class of 1 MW h and batteries on the consumer side are of a class of 10 to several tens kW h. Among them, consumer side batteries has recently attracted much attention since the percent load will be improved by several percents if such a system is provided widely in the order of millions of units [4].

The objective of this work is to develop a large-scale lithium ion battery of 1 kW h class for the power storage. Fundamental studies on reactions in the lithium battery have been done by a large number of researchers, and many reports have been published [5–7].

After starting the R&D of a large-scale lithium ion battery for power storage in 1986, we have prepared the four models of large-scale batteries so far. In this series of work, lithium ion batteries with a capacity of 1 kW h were focused on our efforts improving the durability and efficiency of the 1 kW h battery. For this purpose, test batteries were prepared on the basis of the data accumulated through the past experience as much as possible and were evaluated in their performance. After evaluation, the batteries were dismantled to be examined in their cause of their defects. If problems were so significant that the original design had to be reconsidered, we performed supplementary experiments and prepared the subsequent models on the basis of the results obtained. The target durability of a 1 kW h test model was set at 500 cycles.

This paper summarizes the results of the series of experiments of the first to the fourth model prepared for the long life of a 1 kW h class lithium ion battery.

* Corresponding author. Fax: +81-6-6466-1274.
E-mail address: majima@okk.sei.co.jp (M. Majima).

0378-7753/01/$ – see front matter © 2001 Elsevier Science B.V. All rights reserved.
PII: S0378-7753(00)00507-3

2. Test procedures

2.1. Preparation of electrodes

2.1.1. Cathode

$LiCoO_2$ with a mean particle size of 6.5 μm (Nippon Kagaku Ind., Japan) was used as the cathode active material, carbon black with a mean particle size of about 0.6 μm (Lonza, Switzerland) was used as a conductive agent, PVdF powder (Aujimont, Italy) was used as a binder, and *n*-methyl-2-pyrrolidone was used as a solvent to prepare electrode paste.

The cathode active material, conductive agent, binder, and solvent were mixed at a weight ratio of 10:1:1:5.5 under high purity nitrogen atmosphere for about 1 h. The paste obtained was spread over an aluminum foil of about 20 μm thick by a doctor blade method using an electrode coating machine (Sank, Japan). The paste was applied so that the weight after drying of the electrode would become 0.03 g/cm^2 unless otherwise indicated. The electrode coating machine was designed to pass the paste applied to the foil by doctor blading through a dry atmosphere at 150°C for about 2 min. In this process (primary drying), most of the solvent was eliminated by evaporation. After the passage through the drying furnace, the electrode was wound, stored in an incubator, and the residual solvent and moisture were removed by vacuum drying at 150°C for 4 days (secondary drying). After secondary drying, the electrode was compressed with a roll presser (Sank, Japan) to reduce its thickness to about 80% of the thickness of the active material layer excluding the thickness of the metal foil. After the electrode was cut into a necessary size, it was dried under normal pressure at 150°C for 4 days (tertiary drying) and then was used to prepare a battery.

2.1.2. Anode

Natural graphite with a mean particle size of 12.0 μm (The Kansai Coke and Chemicals, Japan) was used as an anode active material, PVdF powder (Aujimont, Italy) was used as a binder, and special grade *n*-methyl-2-pyrrolidone was used as a solvent to prepare paste. The anode active material, binder, and solvent were mixed at a weight ratio of 10:2:10 and kneaded in a high purity nitrogen atmosphere for about 1 h. The paste obtained was spread over a copper foil about 20 μm thick by doctor blading using an electrode-coating machine (Sank, Japan). The paste was applied so that the weight after drying of the electrode would become 0.01 g/cm^2. The electrode was dried and cut to preparation similar to that of the cathode except that the electrode was compressed to a thickness of about 60% of that of the active material layer excluding the thickness of the metal foil.

2.1.3. Preparation of electrode laminates

The cathode, separator, and anode were layered in this order, and the terminals of every 20 cathode–anode pairs were bound with rivets. They were further layered to a predetermined number, and electrode laminates were obtained. The entire process of layering of electrodes was performed in a dry box containing an atmosphere of 100% argon.

2.2. Electrolyte

The electrolyte was prepared by dissolving 1 M $LiPF_6$ or 1 M $LiBF_4$ (Mitsubishi Chemical, Japan) with a mixture of ethylene carbonate (EC) and diethyl carbonate (DEC).

The mixture of EC and DEC was prepared at a volume ratio of 7:3 unless otherwise indicated. After infusion of the electrolyte, the pressure was reduced to 400 Torr using a pump, and impregnation of the electrolyte was made for 144 h.

2.3. Preparation of coin batteries

For fundamental evaluation of materials, tests using coin batteries were carried out. The cases of the coin batteries consisted of an aluminum lid serving as the cathode, a stainless steel (SUS 304) case serving as the anode, a nickel spacer, and a polyethylene gasket to insulate the lid from the case. A hole of 1 mm in diameter was made in the center of the cathode by removing the active material, and aluminum foil was connected to the lid at this site using a spot welder. The electrode was designed to have an area of 1 cm^2 except for the hole in the center. The anode was prepared by spot welding the nickel spacer to the case material, and then, connecting a copper foil with the nickel spacer. The anode also had an area of 1 cm^2. A polypropylene separator, which was slightly larger than the cathode or anode and 25 μm thick, was inserted between the cathode and anode, and about 0.2 cc of an electrolyte was infused. All procedures were carried out in a dry box containing an argon, in which the moisture was controlled at 0.01 ppm or less. The electrolyte was prepared by dissolving 1 M $LiPF_6$ (Mitsubishi Chemical, Japan) in a 7:3 mixture of EC and DEC unless otherwise indicated. After infusion of the electrolyte, the pressure inside the side box attached to the dry box was reduced to 660 Torr, and electrolyte impregnation was performed for 5 min. The battery case was covered with the lid and sealed with a caulking machine.

2.4. Preparation of single cell batteries

For basic evaluation for scale-up of the battery, single cell batteries with a structure shown in Fig. 1 was evaluated. The cathode and anode, which were cut into a premeditated size, were placed on each side of the separator, sandwiched with fluorine resin plates with a thickness of 3 mm, sandwiched further with SUS 304 plates with a thickness of 10 mm, and these layers were bound with bolts. The number of bolts used varied with the size of the electrodes, but the bolts were tightened with a torque wrench so that a pressure of about 3 kg/cm^2 would be applied to the electrodes. This unit was placed in an SUS 304 case with an interior wall coated with fluorine resin, a predetermined volume of an electrolyte was

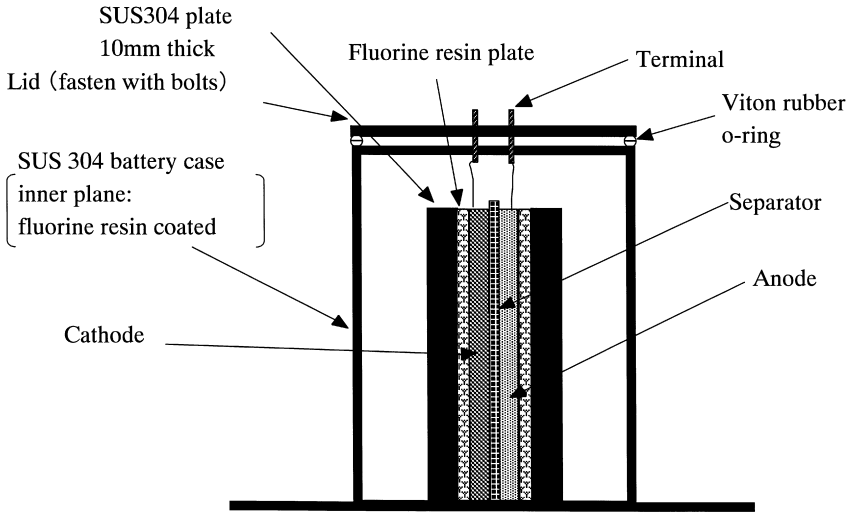

Fig. 1. Schematic illustration of the large-scale single cell system.

infused in a dry box, the lid was closed by interposing an o-ring (Viton), the pressure of the interior was reduced to 660 Torr through the orifice of the safety valve in the lid, and this state was maintained for a predetermined period. The period of decompression was 48 h in the experiments carried out before evaluation of the impregnation time and 144 h in the experiments carried out after evaluation of the impregnation time, unless otherwise stated. After penetration, the lid was opened, the surplus electrolyte was removed, and the cathode and anode were connected to the terminals attached to the lid.

2.5. Assembly of test model

Fig. 2 schematically illustrates the structure of the test battery. The cathode, separator, and anode were layered in this order in a dry box filled with an argon atmosphere, and the laminates were inserted into a battery case. A predetermined volume of the electrolyte was infused into the battery case, the electrodes were impregnated with the electrolyte under a low-pressure condition, and the battery case was sealed. The aluminum collector on the cathode side and the copper collector on the anode side were connected to copper external terminals via wires coated with fluoride resin. The appearance of the battery was basically the same as that of the fourth test model shown in Fig. 3. Table 1 lists the composition of the four test models. The first test model was designed after the composite of a small lithium ion battery and according to our experience in the development of batteries.

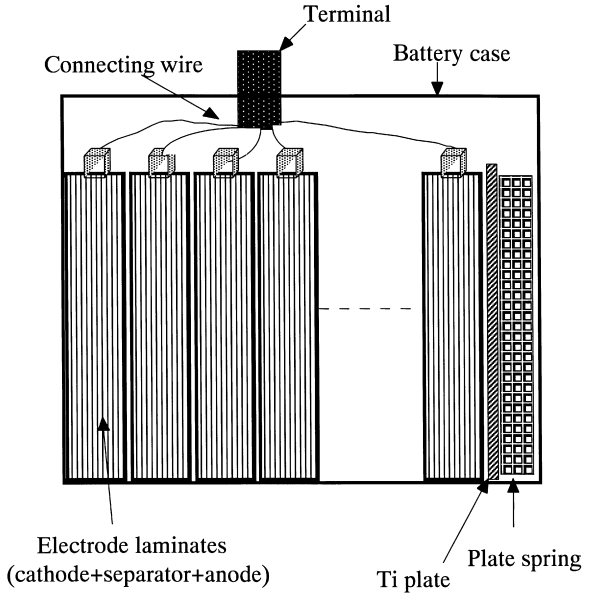

Fig. 2. Schematic illustration of the large-scale lithium ion battery (cross-section).

2.6. Assessment of batteries

The coin batteries and single cell batteries were assessed using an HJ series charge–discharge apparatus (Hokuto

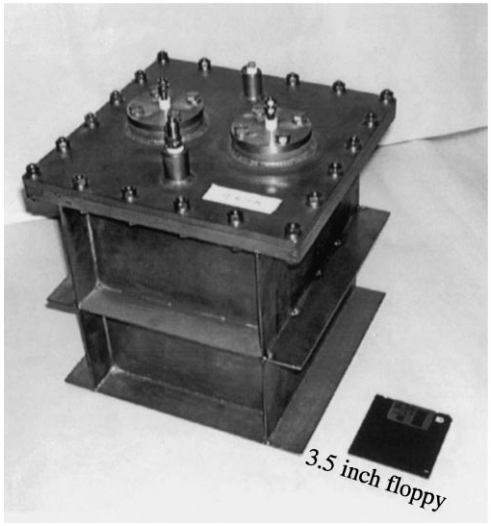

Fig. 3. Appearance of the fourth battery.

Table 1
Composition and performance of the four batteries

	Battery number			
	First	Second	Third	Fourth
Electrode	200 mm×200 mm, 550 cells	170 mm×170 mm, 659 cells	200 mm×200 mm, 725 cells	200 mm×200 mm, 725 cells
Cathode	$LiCoO_2$, particle size 20 μm	$LiCoO_2$, particle size 6.5 μm	$LiCoO_2$, particle size 6.5 μm	$LiCoO_2$, particle size 6.5 μm
Anode	Natural graphite, particle size 12 μm	Natural graphite, particle size 12 μm	Natural graphite, particle size 12 μm	Natural graphite, particle size 12 μm
Drying condition	130°C, 6 h	150°C, 144 h	150°C, 144 h	150°C, 144 h
Collector (thickness)				
Cathode	Al 20 μm	Al 20 μm	Al 20 μm	Al 20 μm
Anode	Cu 20 μm	Cu 20 μm	Cu 20 μm	Cu 20 μm
Electrolyte				
Solute	$LiBF_4$	$LiPF_6$	$LiPF_6$	$LiPF_6$
Solvent	EC:DEC=1:1 (vol.%)	EC:DEC=7:3 (vol.%)	EC:DEC=7:3 (vol.%)	EC:DEC=7:3 (vol.%)
Impregnation condition	660 mmHg, 24 h	660 mmHg, 48 h	660 mmHg, 144 h	400 mmHg, 100 h
Separator (thickness)	PP separator 25 μm	PP separator 25 μm	PP separator 25 μm	PP separator 25 μm
Battery case (thickness)	PE 20 mm	Ti 4 mm	Ti 4 mm	Ti 4 mm
Battery size and weight	L234 mm×W160 mm ×H275 mm, 15 kg	L184 mm×W187 mm ×H248 mm, 10 kg	L210 mm×W210 mm ×H250 mm, 10 kg	L211 mm×W206 mm ×H240 mm, 10 kg

Denko, Japan). Unless otherwise indicated, the batteries were charged at a constant current with a current density of 0.4 mA/cm^2, discharged to 3.0 V at the same current density, and this cycle was repeated. The maximum voltage was 4.2 V, and the end point of the battery life was evaluated according to the degree of elevation of the charge end voltage.

2.7. Methods for evaluation of characteristics of test models

Evaluation of the performance of the fourth model was made using a BS2500 series charge–discharge apparatus (Keisokuki Center, Ltd., Japan). The methods for evaluation are shown in Table 2. The battery was charged at a current density of 0.15 mA/cm^2 and a maximum voltage of 4.1 V for 8–10 h under a constant current–constant voltage (CC–CV) condition, and discharged at the same current density to 3.0 V, and this cycle was repeated. It was charged under a CC condition at a current density of 0.15 mA/cm^2 for 8 h and at the maximum voltage of 4.3 V, and the durability of the battery was evaluated according to the increase in the charge end voltage. With the third test model, the maximum voltage was increased from 4.1 to 4.15 V after the 250th cycle to determine the optimal maximum voltage in a large-scale battery.

3. Analysis of problems revealed by fundamental experiments and evaluation of test batteries — test results and discussion

3.1. Fundamental evaluation before preparation of the first model

Before preparation of the first test model, the following problems were evaluated. Naturally, some of these problems need evaluation also in designing small batteries.

Table 2
Evaluation methods for test batteries

Assessment	Battery number			
	First	Second	Third	Fourth
Battery test conditions	Charge: 0.15 mA/cm^2, limit 4.3 V Discharge: 0.15 mA/cm^2, limit 3.0 V	Charge: 0.15 mA/cm^2, limit 4.36 V Discharge: 0.15 mA/cm^2, limit 3.0 V	Charge: 0.15 mA/cm^2, limit 4.1 V(CC–CV) Discharge: 015 mA/cm^2, limit 3.0 V	Charge: 0.15 mA/cm^2, limit 4.1 V(CC–CV) Discharge: 0.15 mA/cm^2, limit 3.0 V
Remarks	Maximum capacity test: fifth cycle Self discharge test: 40th cycle	Maximum capacity test: eighth cycle	Maximum capacity test: eighth cycle Charge limit 4.15 V: after 250th cycle	Maximum capacity test: eighth cycle

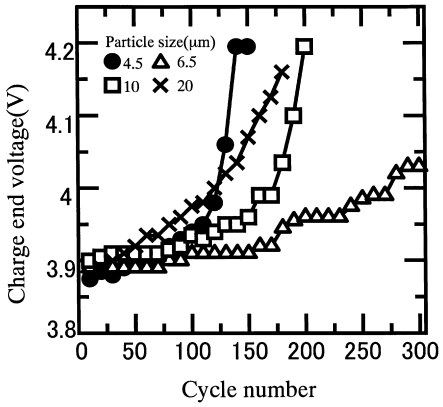

Fig. 4. Effect of the particle size of cathode active material on cell resistance.

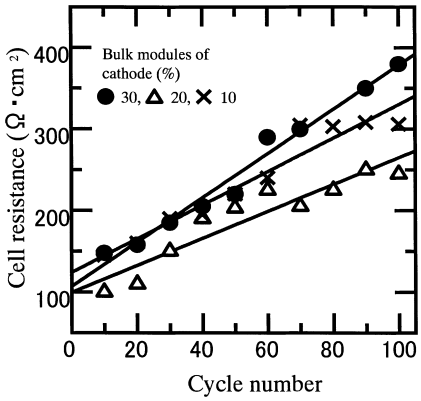

Fig. 5. Effect of bulk modules of cathode on cell resistance.

3.1.1. Particle size of electrode active materials

Fig. 4 shows the results of experiments. The increase in cell resistance with repetition of cycles was found to be smallest when the mean particle size was 6.5 μm. Therefore, the active materials were prepared at a mean particle size of 6.5 μm for large-scale batteries. From the results shown in Fig. 4, we considered that the particle size of the electrode active materials is closely related to the effective surface area of the electrodes, i.e. it has a major effect on the interface between the electrolytic solution and the active material. As the particle size decreases, and as the effective surface area increases, the influx and outflux of Li^+ ion increases, and the cell resistance decreases at a fixed current density. However, adverse effects of reducing the particle size are also expected. If the active materials are deteriorated by insertion and release of Li^+ ion, points of deterioration increase as the particle size is smaller so that the cell resistance is increased. This suggests the presence of an optimal particle size in the active material. However, the mixing of active materials with different sizes may improve the battery performance considerably.

A similar test was performed concerning natural graphite used as the anode. Since no marked difference was observed unlike the cathode, evaluation of the particle size of the anode active material is omitted here.

3.1.2. Electrode compression rate

Effects of the compression of electrodes during their preparation were evaluated. The cathode and anode were compressed separately, and the effects of the compression rate on the cell resistance were evaluated. Fig. 5 shows the results of experiments concerning the cathode. In the cathode, if the compression of the active material is insufficient, the electric contact resistance between the active materials is increased. If, on the other hand, excessive compression is applied, the space into which the electrolyte can penetrate is reduced, and the cell resistance is increased, with consequent interference of the reaction. As is clearly indicated by the figure, a compression rate of 20% is considered to be optimal for the cathode.

Similar measurements were performed also in the anode. The optimal compression rate for the anode was found 40%. This is considered to be related to the fact that natural graphite used as the anode active material showed greater expansion than the cathode active material.

3.2. Analysis of problems observed in the first test model

Problems disclosed in the first model included: (1) the kind of electrolyte and the composition of the solvent; (2) the compression structure of the electrode laminates, materials of the battery case, electrode area, and sealing properties of the case; and (3) drying conditions of the electrodes.

3.2.1. Kind of electrolyte and composition of solvent

In the first model, 1 M $LiBF_4$-EC/DEC was used as the electrolyte. When this electrolyte was used, the current efficiency was not stabilized until about the 20th cycle and reached only 98% even in the 30th cycle. When the electrolyte was changed to 1 M $LiPF_6$-EC/DEC, the current efficiency reached 100% after a few cycles and remained stable thereafter.

In small batteries, a mixture of EC and DEC is often used as a solvent for 1 M electrolyte [8]. EC has a high permittivity and tends to dissociate $LiPF_6$ into Li^+ and PF_6^-. Since EC is solid at room temperature, it must be mixed with DEC, which is a low viscosity solvent. The ion conductivity of EC/DEC is known to be greatest when the volume percentage of DEC is 50%, and an electrolyte with this composition is often used in small batteries. To examine whether this composition is suitable for a large-scale battery with a large capacity, the charge end voltage–cycle curve was examined by changing the composition of the EC/DEC mixture. Fig. 6 shows the results. As is clearly observed in the figure, a DEC content of 30% is considered to be the optimal in a 1 M $LiPF_6$-EC/DEC electrolytic solution for the durability of a

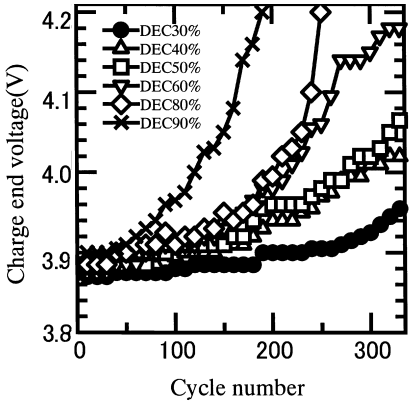

Fig. 6. Effect of EC/DEC mixing ratio on 1 M $LiPF_6$ electrolyte.

large lithium ion battery. Since the viscosity of the electrolytic solution becomes excessive when the DEC content <30 vol.%, the second test model was prepared using a mixture of EC and DEC at a volume ratio of 70:30.

3.2.2. Compression structure of the electrode laminates, case material, electrode area, and sealing properties of the case

Many fragments of cathode and anode active materials were observed inside the case of the battery when it was dismantled. In the first test model, the battery case was made of polyethylene, but the case was deformed in the direction of lamination because of insufficient strength. In $LiCoO_2$/graphite batteries, the electrodes are known to expand and contract during charging and discharging. Therefore, we evaluated installation an appropriate buffer material and changing the case material from PE to Ti, which is stronger and resistant to corrosion. Since no report was available then on the expansion and contraction of the electrode laminates, we prepared Ti plate springs and used them in a newer model.

Effects of the electrode size on charging and discharging were studied using single cells of 14 cm×14 cm, 17 cm×17 cm and 20 cm×20 cm, as shown in Fig. 7, and

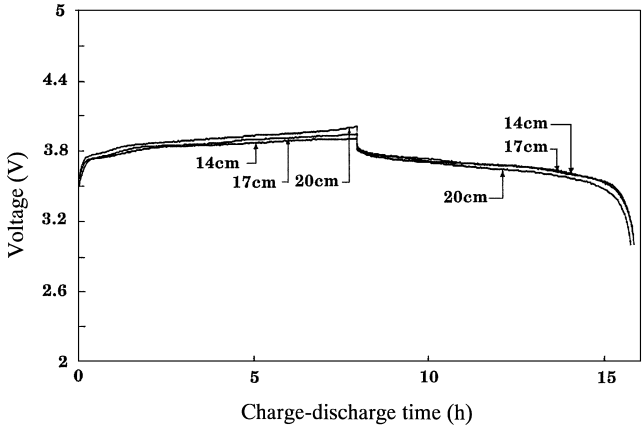

Fig. 7. Influence of electrode size on charge–discharge voltage.

conditions that minimize the cell resistance were evaluated. As indicated by the figure, the voltage difference between charging and discharging, i.e. the cell resistance slightly increased with the electrode area. This increase in the cell resistance is considered to be ascribed to the increase in the heterogeneity of the electrodes with the increasing electrode size. Although the cell resistance was minimum in the 14 cm×14 cm electrode, an excessive number of laminate were needed to obtain a capacity of 1 kW h, so that the electrode area was set at 17 cm×17 cm or 20 cm×20 cm.

In the lithium ion battery, entry of moisture from outside and loss of the organic electrolyte by evaporation from the case are considered to be significant causes of the decrease in its performance. Therefore, we evaluated the sealing property of the case. Three sealants, i.e. (1) the Viton rubber o-ring; (2) flat metal packing; and (3) PTFE tape, were examined for use between the case and the lid. The Viton o-ring was selected, because it was found to be superior in the ability to prevent both the entry of moisture from outside and leakage of the electrolyte from inside.

3.2.3. Drying conditions of electrodes

The assembling process of a large battery is considerably more complicated than that of a small battery. Restriction of the entry of moisture is a factor that needs particular attention in the assembling process. Since moisture is considered to have a major effect on the durability of the battery, we evaluated the drying method for the electrodes. The charge end voltage increased when the drying temperature was too high or too low to the disadvantage of prolongation of the battery life. Under the conditions of this study, the charge end voltage was lowest when the drying temperature was 150°C. The electrodes were prepared by mixing the active material with a binder and making the mixture paste-like with a pyrrolidone solvent. From the viewpoint of elimination of moisture, a higher drying temperature is more advantageous. However, the melting point of the binder used for preparation of the electrodes is 177°C so that partial melting may occur and cause an increase in the charge end voltage when the electrodes are dried at 170°C. Also, there is the report that the crystalline particle size of the binder in the paste is maximized around 142°C and that the small particle size of the binder is advantageous for prolongation of the battery life [9]. These findings may explain the results of our study indicating the presence of the optimal drying temperature around 150°C. Therefore, the electrodes were dried at 150°C for preparation of the subsequent models.

Moreover, as the solubility of water in the pyrrolidone solvent is extremely large, the presence of residual pyrrolidone in the electrode is considered to allow entry of moisture from outside in the subsequent assembly processes even if moisture can be eliminated in the drying process. Fig. 8 shows serial changes in the water content of the electrode according to the content of residual pyrrolidone. The results established the validity of the above hypothesis.

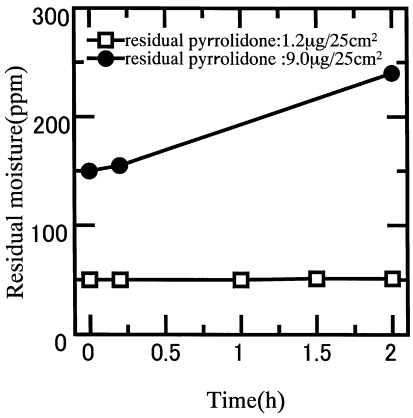

Fig. 8. Time variation of water content in electrodes with different residual pyrrolidone contents.

3.3. Analysis of problems observed in the second test model

The problems included (1) the effects of the use of plate springs; (2) penetration conditions of the electrolyte; and (3) thickness of the collectors.

3.3.1. Effects of the use of plate springs

In the second test model, plate springs made of Ti 15 cm long, 10 cm wide, 1.7 cm wide, and 0.3 cm thick with a shape shown in Fig. 9 were used. When the second model was dismantled, no loss of the electrode active materials as observed in the first model was noted, and the use of the Ti plate springs was considered to be effective for prolonging the battery life. However, as the design of the plate springs used in this model had no theoretical grounds, we measured expansion and contraction of the electrodes associated with charging and discharging and designed plate springs for subsequent models on the basis of the results obtained. The results were reported elsewhere [10].

3.3.2. Optimization of impregnation conditions of the electrolyte

As observed above, the results of this study suggested that the battery reaction becomes more uneven as the electrode area increases. Therefore, a single cell battery with an electrode size of 17 cm×17 cm was charged and discharged over 10 cycles at a current density of 0.15 mA/cm^2, the cathode and anode were equally divided into nine parts, both longitudinally and horizontally after the test, and the Li content of each segment was assayed by measuring inductively coupled plasma (ICP). Li was found to be present in relatively large amounts on the left and right sides of the lower margin of the electrodes. Such uneven distribution of Li was estimated to be a result of inadequate impregnation of the electrolyte.

In this study, the electrolyte was impregnated as follows. After the electrode laminates were placed in the battery case, the electrolyte was infused, and the lid was closed. Then the pressure inside the battery case was reduced to 660 Torr (atmospheric pressure is 760 Torr), and the case was allowed to stand in this state for 24 h. If impregnation of the electrolyte into the electrodes is insufficient, uneven reactions are considered to occur on the surface of the electrodes. Therefore, we assembled single cell batteries with electrode sizes of 10 cm×10 cm and 17 cm×17 cm, impregnated the electrodes with the electrolyte at 660 Torr for various durations, charged and discharged the batteries repeatedly at a constant current density of 0.15 mA/cm^2, and measured the cell resistance in the 10th cycle.

Fig. 10 shows the results. In sample with a smaller electrode area, the cell resistance approached the intrinsic value of the electrode after impregnation for 1 h. However, in sample with a larger electrode area, the cell resistance was high while the impregnation time was short, but it became comparable to that of smaller sample after impregnation for 100 h. When the cell resistance value in sample with small area after impregnation for 100 h was assumed to be the intrinsic cell resistance of this battery, the time needed for sample having large area was estimated to be 144 h by extrapolation.

Impregnation of electrodes with the electrolyte is expected to be closely affected by the internal pressure of the battery. In fact, impregnation of the electrolyte is made near 0 Torr in small commercial batteries. Therefore, an experiment was carried out using a single cell battery with an electrode size of 17 cm×17 cm at a fixed impregnation

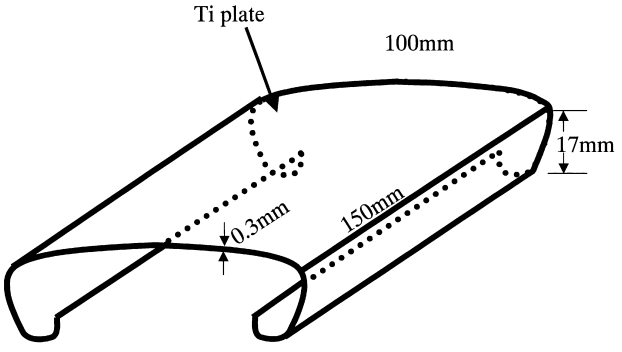

Fig. 9. Schematic illustration of Ti plate spring.

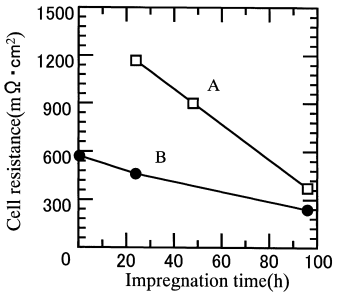

Fig. 10. Effect of impregnation time in cell resistance for the electrode system using different electrode sizes (A: 17 cm×17 cm, B: 10 cm×10 cm, impregnation pressure: 660 Torr).

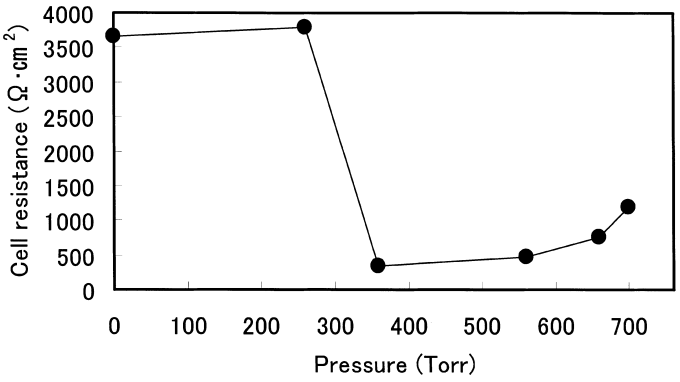

Fig. 11. Effect of impregnation pressure on the cell resistance of a single cell using 17 cm×17 cm electrodes (impregnation time: 96 h).

time of 96 h by changing the pressure during impregnation. The results are shown in Fig. 11. The cell resistance decreased slightly as the impregnation pressure was reduced from 700 to 360 Torr, and approached the intrinsic cell resistance of the battery. However, as indicated in the figure, the cell resistance increased rapidly as the pressure is reduced below 300 Torr. We had confirmed in a preliminary evaluation that the electrolytic solution boils at about 300 Torr at a temperature of 297 K, being consistent with the results shown in Fig. 11. Prolonged impregnation under a markedly reduced pressure may cause bubbles on the surface of the electrodes and inhibit homogeneous impregnation, contributing to increases in the cell resistance.

Either electrode shown in Fig. 10, the electrode area was markedly greater than in any small battery, but the cell resistance was already close to the intrinsic value immediately after the beginning of impregnation. Therefore, impregnation is considered to progress nearly instantaneously in small batteries. This is probably why impregnation can be made adequately in small batteries by infusing a small volume of an electrolytic solution over a very short period into the battery after decompression to nearly 0 Torr. In contrast, as indicated by the results shown in Figs. 10 and 11, homogeneous impregnation of electrodes with an electrolyte becomes an extremely difficult process as the electrode size increases. In large batteries, in which large electrodes are laminated, impregnation under moderate decompression and over a sufficient period is considered to be of particular importance.

3.3.3. Effects of thickness of copper foil as the anode collector on cell resistance

A copper foil was used as the anode collector, but examination of the second test model by dismantling revealed that contact between natural graphite, which is the anode active material, and the kneaded binder was inadequate. The tightness of contact was evaluated by the X-cut tape test of the Japan Industrial Standards (JIS). As a result, the tightness of contact was considered to be dependent on the electrode compression method, i.e. it is closely related to expansion and contraction of the electrode associated with charging and discharging. Therefore, we studied the cell resistance–cycle curve at two levels of copper foil thickness, i.e. 20 and 40 μm. In this study, the compression rate of the anode was 40%. The cell resistance was markedly reduced by doubling the copper foil thickness to 40 μm. On the basis of these findings, we used a 40 μm thick copper foil as the anode collector in the third test model. However, since contact was shown by subsequent evaluations to be improved also by the use of a frame to prevent the occurrence of stress in the compression process to a similar degree to increasing the copper foil thickness, the thickness of the copper foil used in the fourth test model was returned to 20 μm.

3.4. Analysis of problems in the third model

Problems revealed in the third test model included: (1) contact of the active material on the surface of the collector; (2) treatment of the anode edge; (3) uniformity of the electrode thickness; (4) treatment of electrode terminals; and (5) charging method and maximum charging voltage.

3.4.1. Improvement in contact of active materials

In large capacity laminated batteries, the electrodes expand and contract during charging and discharging, respectively. These expansion and contraction are too large to be ignored and cause deformation of electrodes to an irreparable extent, resulting in heterogeneous battery reaction and a short battery life, unless appropriate preventive measures are taken. With the objective of reducing such deformation to 0.1 mm or less, we designed a wavy plate spring using computer simulation based on the limited factors method. The results were summarized elsewhere [10].

3.4.2. Treatment of anode edges

On examination of the third model by dismantling, a dendritic gray precipitate was observed at edges of the anode, particularly at the left and right lower edges. This abnormal precipitation of Li is estimated to be a result of concentration of electrolysis at the edges of the electrode and consequent prevention of uniform reaction. We, therefore, coated the lower part and the left and right edges of the anode with a paste of the active material kneaded with an increased percentage of the binder and showed that this method is useful for the prevention of precipitation of Li dendrites. As shown in Fig. 12, the increase in the cell resistance associated with the increase in the number of cycles was markedly slowed when the anode was treated by this method.

3.4.3. Prevention of uneven reaction on the electrode surface

Increasing the electrode area is a reasonable method for increasing the capacity of the battery, but measures to improve the precision of preparation of the electrodes and

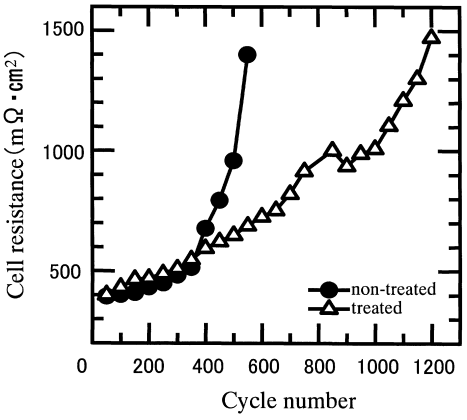

Fig. 12. Prevention of dendrite formation by edge treatment of the anode.

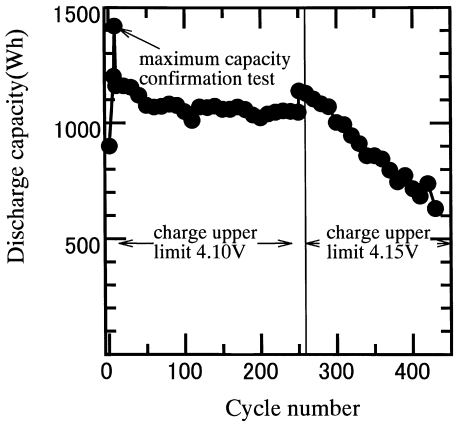

Fig. 13. Life estimation test done for the third battery (blank circles indicate the results obtained of a single cell battery with 17 cm×17 cm electrodes).

to reduce the effects of the electrode area are also considered to be important. We, therefore, evaluated methods to reduce the variation in the electrode thickness. The active materials were applied to the collector foils by the doctor blading method. The variation of the electrode thickness could be reduced from ±10 to ±5 μm or less by stabilizing the coating speed and improving the mirror surface quality of the role used for role pressing of the electrodes. A charge–discharge test was performed using electrodes with reduced variation in thickness in a single cell, and a variation in the thickness of about 5 μm was shown not to exert marked effects in a single cell battery. However, in a large battery, in which several hundreds of electrodes are laminated, this reduction in the variation of electrode thickness is considered to have had a major effect with regard to even weight-bearing and even electrolyte impregnation.

3.4.4. Prevention of corrosion of terminals

When the battery was dismantled, marked discoloration was observed in the septum near the electrode terminals, elements considered to have been derived from corrosion of the terminals were detected in the residual fluid in the battery case, and corrosion of the surface of terminals was grossly evident. To prevent corrosion of the terminals, the terminal size was reduced from 3 cm×4 cm to 1.5 cm×4 cm, and the number of rivet connection points was increased from one to two, in the fourth test model.

3.4.5. Effects of changes in the charge end voltage on the battery life

In the performance test of the third test model of large-scale lithium battery, charging and discharging were repeated at a charge end voltage of 4.10 V over 250 cycles and at 4.15 V in the subsequent cycles. In this test, significant differences were observed in the capacity–cycle curve after the charge end voltage was altered, and the battery life ended after 460 cycles, as shown in Fig. 13. The battery life would have been greatly extended if the charge end voltage had been maintained at 4.10 V and the tendency of changes in the capacity observed to the 250th cycle had been sustained.

To examine whether such a change in the charge end voltage in the middle of a test affects capacity–cycle characteristics or not, we prepared a single cell with 17 cm×17 cm electrodes and charged and discharged the battery at a charge end voltage of 4.10 V in the first 200 cycles and 4.20 V in the following cycles. The results obtained are demonstrated in Fig. 14. As indicated by the figure, no significant change was observed despite the change in the charge end voltage. While the third test model was a laminated battery with 725 cells, a single cell was examined in this test. However, there was no basic difference in the capacity–cycle curve between these batteries up to the 200th cycle as observed in Fig. 14. This suggests that the laminated structure of the battery is unlikely to be the direct cause of the difference in the capacity–cycle profile. More precise control of the voltage unit may have been needed also in the third test model. Paying attention to this point, we carried out subsequent test at a charge end voltage of 4.10 V. The problem of precision of voltage control by the voltage unit will be encountered at the stage of practical application of the battery.

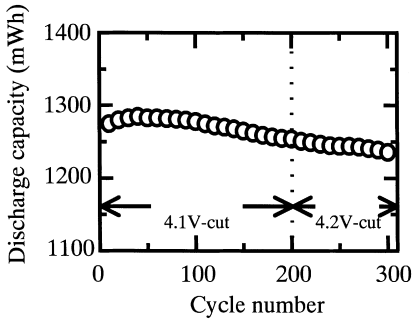

Fig. 14. Effect of the change in charge end voltage during charge–discharge test on discharge capacity (electrode size: 17 cm×17 cm).

3.5. Analysis of problems in the fourth test model

The fourth test model was recently dismantled, and factors in deterioration of the capacity were evaluated.

On observation of the surface of the electrodes, discoloration estimated to be due to precipitation of EC was noted in the cathode, but parts of brown discoloration and parts of blue discoloration were observed, and the golden color characteristic of Li was lost, in the anode. When the Li and Co contents of the cathode made of $LixCoO_2$ per 20 electrodes were examined by the luminescence assay technique, there were areas with x-values of 1 or less in the center of the electrode stack, and the x-value showed a clear variation. However, the variation was markedly smaller in the fourth model than in the third model. This reduced variation is considered to be due to (1) fixation of the charge end voltage at 4.10 V; (2) control of generation of inactive Li by treatment of the anode edges; and (3) uniform compression achieved due to the absence of marked deterioration of the plate springs. Major factors in deterioration of the fourth model are estimated to have been an increase in the internal resistance due to closure of the septum by degradation products of the electrolyte and disturbance of the capacity balance between the cathode and anode. X-ray diffraction analysis of the discolored area in the anode revealed peaks considered to represent LiC_6, LiC_{12}, and LiC_{24} as well as natural graphite.

On observation of the surface of the septum in the dismantled battery, little precipitate was generated in the areas that showed no discoloration even in enlarged photographs. In the areas that showed brown discoloration, no marked deterioration such as changes and destruction of the membrane structure was noted, but a large number of capsule-like precipitates considered to be degradation products of the electrolyte were observed, and they were seen to obstruct pores in the septum. The precipitates were identified by energy dispersion X-ray spectrophotometry to be Co, C, P, F and Cu derived from the cathode active material, anode active material, electrolyte, and anode collector, respectively. Staining considered to be due to deposition of materials released from the cathode and anode active materials was also noted. Since more capsule-like precipitates and deposits of materials released from the electrode active materials were observed in the fourth test model than in the third test model, an increase in the internal resistance due to clogging of degeneration products of the electrolyte and a reduction in the capacity due to loss of active materials are estimated to have occurred simultaneously.

The septum was removed at every 20 electrodes, the electrolyte contained in the septum was extracted with acetone, and changes in the EC/DEC ratio=Y-value and qualitative analysis of other components were carried out by gas chromatography. Part of DEC, a solvent with a low boiling point, is considered to have evaporated during impregnation of the electrolytic solution and preparation of samples, but the Y-value was slightly smaller in the fourth test model than in the third test model. The electrolytic solution remaining in the bottom of the battery case was collected and analyzed by ICP, and the presence of Li, P, Ti, Co, Cu, Si, Fe, Al, and Sn was confirmed. Quantitative analysis was impossible because of the limitation of the sample volume. The elements other than those contained in the electrode active materials, electrolytic solution, battery case, electrolyte, and collector are considered to have been derived from corroded terminals.

In the third test model, marked brown discoloration was observed in the septum near the cathode terminal, but such marked discoloration was not observed in the fourth model. However, photographic examination of the cathode and anode terminals showed discoloration in the terminal of the Al collector of the cathode. The resistance of the terminal measured at 1A was initially 4.10×10^{-3} and 0.50×10^{-3} mΩ in the cathode and anode, respectively, but it was increased to 6.45×10^{-3} and 1.20×10^{-3} mΩ, respectively, at dismantling. In lithium ion batteries, corrosion of the terminals by hydrofluoric acid caused by the reaction between the electrolyte and water can pose a problem. Therefore, we performed composition analysis of the gas collected during dismantling of the fourth test model. Although information concerning gases containing four or more carbon atoms could not be obtained due to the limitation of the ability of the analytical apparatus, but the volume percentages of components were 0.8 for H_2, 0.003 for CO, 8.33 for CO_2, 0.18 for CH_4, 0.022 for C_2H_6, 0.14 for C_2H_4, and 0.001 for C_3H_8, with the rest consisting of N_2, O_2, and Ar. The quantities of major components were CO_2>H_2>CH_4>C_2H_4. In the third test model, no particular difference was observed in the composition of gases except that the quantities of C_2H_2 and C_2H_4 were C_2H_2>C_2H_4.

4. Evaluation of performance of test batteries

The four test batteries were fabricated as detailed in Table 1 and evaluations of battery performance were conducted according to the methods shown in Table 2.

On the occasion of trial manufacturing of the first battery, we mainly used the data reported on the small-sized lithium ion batteries. With the first battery, a maximum capacity confirmation test was performed at the fifth cycle, and the maximum capacity was 1145 W h. A self-discharge test was performed at the 40th cycle, and a large of self-discharge rate of 19% per week was obtained. The capacity became <70% of the baseline level at the 50th cycle, when the life of the battery was judged to have ended. The cause of the large self-discharge rate was estimated to be the use of natural graphite as the anode active material. The energy efficiency was high at 86.6% already in the first cycle, but it was low at the maximum capacity confirmation test and at self-discharge test. The energy density was 60 W h/kg on the weight base and 111 W h/l on the volume base.

Table 3
Performance of the four batteries

Performance	Battery number			
	First	Second	Third	Fourth
Capacity (W h)	1147	1134	1420	1595
Cycle life (cycles)	50	245	370	543
Energy density (W h/kg, W h/l)	60, 111	61.7, 133	71.0, 129	79.8, 153
Efficiency (energy efficiency in %)	80	85	85	85

Since the above results indicated that the short life of the battery was a problem with the first model, and the cause of the short life was evaluated by careful observation of dismantled battery to provide useful grounds for the design of the second battery. As is clear in Table 3, battery life, energy efficiency, energy density, and capacity steadily increased as the trial manufacturing advanced. Energy density on the volume base obtained in these test batteries were still low, but it may be improved by using suitable anode active materials such as MCMB (mesophase carbon micro beads) or $Li_{4/3}Ti_{5/3}O_4$ instead of natural graphite, to eliminate the effect of expansion and contraction caused but charging and discharging the battery. Although the battery life of the first battery was 50 cycles, that of the fourth battery was 543 cycles, as shown in Fig. 15(A).

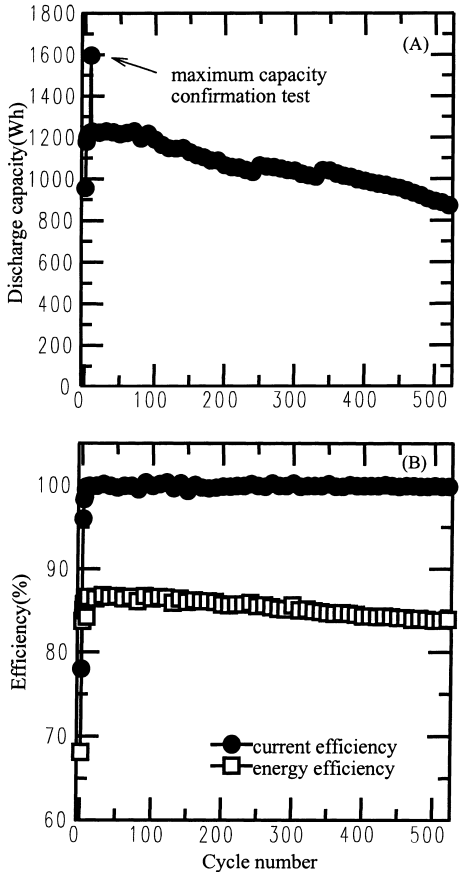

Fig. 15. Battery life estimation test (A) and efficiency change (B) of the fourth battery.

The maximum capacity confirmation test of the fourth battery was performed in the eighth cycle, and a maximum capacity of 1595 W h was obtained. The life span of the battery was 543 cycles, which exceeded the target of 500 cycles. Both of these values surpassed those of the third test model.

Fig. 15(B) shows changes in the efficiency of the battery. While the current efficiency remained about 100%, the energy efficiency decreased linearly from an initial level of 86%. However, the rate of decrease was smaller than in the second or third model, and the energy efficiency remained above 80% even at the 400th cycle.

The energy density on the weight base was 79.8 W h/kg when a light case was used and 69.3 W h/kg when a normal case was used. That on the volume base was 153 W h/l.

As mentioned above, the durability of the battery exceeded the target durability of 500 cycles for the first time in this model.

5. Conclusions

To develop a long-life and high-efficiency large-scale lithium ion battery of 1 kW h class for power storage, $LiCoO_2$ and natural graphite were used as cathode and anode active materials, respectively, and 1 M $LiPF_6$-EC/DEC was used as the electrolytic solution. Basic evaluations of problems were repeated by dismantling the batteries that reached the end of their life, and newer models were prepared with modification in the composition of the battery. We conducted basic evaluations various factors that pose problems in designing a large battery consisting of laminated large electrodes. As a result, factors necessary for uniform progression of electrochemical reactions were shown to have great significance as might be expected. The durability and efficiency could be improved in each model, and high efficiency and a life span of more than 500 cycles, which was the target durability in this project, could be achieved in the fourth model. The performance of this battery was confirmed to exceed that of a commercial lead battery in durability, efficiency, and energy density. We will continue further studies to improve the durability and energy density on volume basis of the battery.

Through preparation of these test models, it was realized that technological factors such as uniform penetration of laminated electrodes with the electrolyte and maintenance of

the state of even compression by controlling the expansion and contraction associated with charging and discharge bear particular importance.

References

[1] T. Sekine, K. Takahashi, Denkigakkai Zasshi 112 (1992) 582.
[2] Outline of Electricity Demand, The Agency of Resources and Energy, Japan, 1991, p. 7.
[3] Y. Suzuki, K. Ito (Eds.), Energy Storage System, Energy and Resources Society of Japan, 1992, p. 3.
[4] R. Ishikawa, Kobunshi 44 (1995) 78.
[5] T. Ohzuku, A. Ueda, M. Nagayama, J. Electrochem. Soc. 140 (1993) 1862.
[6] J.R. Dahn, U. von Sacken, C.A. Michal, Solid State Ionics 44 (1994) 87.
[7] J.N. Dahn, J. Electrochem. Soc. 139 (1992) 2091.
[8] S.T. Mayer, H.C. Yoon, C. Bragg, J.H. Lee, in: Proceedings of the 13th International Seminar on Primary and Second Battery Technology Applications, 1996, 247 pp.
[9] S. Sugawara, Text of Battery Technology and Material, Denkikagaku Seminar (1996) 71.
[10] M. Majima, S. Ujiie, E. Yagasaki, S. Inazawa, K. Miyazaki, J. Power Sources 81/82 (1999) 877.